

J. RYS\*, M. WITKOWSKA\*

## THE EFFECT OF STARTING ORIENTATIONS AND INITIAL MORPHOLOGY ON TEXTURE FORMATION IN DUPLEX STEEL SAF 2205

## WPLYW ORIENTACJI POCZĄTKOWYCH I MORFOLOGII WYJŚCIOWEJ NA TWORZENIE SIĘ TEKSTURY W STALI DUPLEX SAF 2205

The present investigations concern the rolling texture formation and changes in morphology of two-phase structure in cold-rolled mid-alloy duplex stainless steel SAF 2205 with addition of nitrogen. The preliminary thermo-mechanical treatment included hot-rolling with subsequent solution annealing at the temperature 1150°C. Afterwards the steel was cold-rolled within the wide range of reductions by applying two different variants, with rolling directions perpendicular and parallel to the direction of hot-deformation.

Texture analysis indicates that austenite shows tendency to develop the textures similar to those in one-phase austenitic steels regardless of the applied cold-rolling variant and the final rolling textures of ferrite significantly differ from the typical textures of ferritic steels. Formation of the texture close to the  $\{110\}\langle 112 \rangle$  alloy-type texture was observed in austenite and the orientation changes proceeded gradually over a wide range of reductions, especially for the cold-rolling variant perpendicular to the direction of hot-deformation. On the other hand the major component of the ferrite starting texture, i.e. the rotated cubic orientation  $\{001\}\langle 110 \rangle$  and the character of texture spread, which is different for both rolling variants, remained essentially unchanged up to high deformations. It is concluded that the starting orientations of both constituent phases after the preliminary treatment and the band-like morphology of the ferrite-austenite structure considerably influence formation of the cold-rolling textures in the examined duplex type steel.

*Keywords:* duplex stainless steel, nitrogen addition, cold-rolling deformation, initial orientation distribution, ferrite and austenite rolling textures, two-phase morphology

Prezentowane badania dotyczą rozwoju tekstur walcowania i zmian morfologii struktury dwufazowej w walcowanej na zimno średnio-stopowej nierdzewnej stali duplex w gatunku SAF 2205 z dodatkiem azotu. Wstępna obróbka cieplno-mechaniczna obejmowała walcowanie na gorąco oraz wyżarzanie i przesycaanie z temperatury 1150°C. Stal poddano następnie walcowaniu na zimno w szerokim zakresie deformacji, stosując dwa różne warianty z kierunkami walcowania prostopadłym i równoległym do kierunku odkształcenia na gorąco.

Analiza tekstur wskazuje, że niezależnie od zastosowanego wariantu walcowania na zimno austenit wykazuje tendencje do tworzenia tekstur odpowiadających tym w jednofazowych stalach austenicznych natomiast końcowe tekstury walcowania ferrytu różnią się istotnie od typowych tekstur stali ferrytycznych. W austenicie obserwuje się rozwój tekstur zbliżonych do tekstury typu stopu  $\{110\}\langle 112 \rangle$ , a w przypadku wariantu walcowania na zimno prostopadle do kierunku odkształcenia na gorąco zmiany orientacji zachodzą stopniowo w szerokim zakresie odkształceń. Z kolei główna składowa tekstury początkowej ferrytu, tzn. orientacja skręcona sześcienna  $\{001\}\langle 110 \rangle$  jak również charakter rozmycia tekstury ferrytu, odmienny dla obu wariantów walcowania, pozostają zasadniczo nie zmienione do wysokich odkształceń. Należy stwierdzić, że orientacje początkowe obu faz po obróbce wstępnej oraz pasmowa morfologia ferrytu i austenitu wywierają istotny wpływ na tworzenie się tekstur odkształcenia podczas walcowania na zimno badanej stali typu duplex.

### 1. Introduction

The major part of products manufactured of duplex stainless steels is plastically deformed and annealed upon the production process and one of the first manufacturing steps is usually rolling deformation. Plastic deforma-

tion of ferritic-austenitic steels of duplex type is rather complex due to the two-phase character of the structure and the presence of the  $(\alpha/\gamma)$  interfaces, which considerably affect deformation behaviour of constituent phases [1÷3]. Both phases are plastically deformed in the course of hot- and cold-rolling. The formation and subsequent

\* DEPARTMENT OF PHYSICAL AND POWDER METALLURGY, AGH UNIVERSITY OF SCIENCE AND TECHNOLOGY, 30-059 KRAKÓW, 30 MICKIEWICZA AV., POLAND

reduction in thickness of the ferrite and austenite bands result in so-called “pancake” structure. As a consequence the ( $\alpha/\gamma$ ) phase interfaces, which are strong obstacles for dislocation motion, are laying mostly parallel to the rolling plane [1÷6]. From a number of investigations it results that the anisotropy in mechanical properties of duplex steel sheets is not only the effect of a specific morphology of the ( $\alpha/\gamma$ ) two-phase structure but also depends on the crystallographic textures of the constituent phases [7÷9]. The specific band-like morphology of the ferrite-austenite structure creates different conditions for plastic deformation due to the interaction of both phases and considerably constrained lattice rotations. That is why the mechanisms governing the formation of ferrite and austenite rolling textures in duplex steels are supposed to change in comparison to single phase steels [10, 11]. The occurrence of strong initial textures of both component phases after a preliminary treatment and the specific crystallographic orientation relation may additionally affect deformation behaviour in the course of cold-rolling, changing a development and a character of the final rolling textures of ferrite and austenite [4, 5]. Since hot-deformation and subsequent solution treatment produce preferred orientation distributions of the constituent phases, thus conditions of both processes are very important not only from the view point of phase composition and two-phase morphology but also starting textures for further cold-rolling. That is why the initial morphology and the starting orientation distributions of the constituent phases after thermo-mechanical pre-treatment become very important factors, which should be taken into account when analysing texture formation of cold-rolled duplex type steels [4÷6].

The aim of the present research was to examine the effect of the initial ferrite-austenite morphology and the starting orientation distributions, resulting from the change of rolling direction, on a development of the ferrite and austenite deformation textures in duplex steel sheets. Cold-rolling deformation was conducted after the preliminary treatment within the wide range of reductions perpendicularly and parallel to the hot-rolling direction. The volume fractions of the constituent phases after the thermo-mechanical pre-treatment and the alloying addition of nitrogen were also taken into account [12]. The final rolling textures were compared with those for one-phase ferritic and austenitic steels [10, 11].

## 2. Material and experimental procedure

The material under examination was the nitrogen alloyed ferritic-austenitic stainless steel of duplex type X2CrNiMoN22-6-3. Its chemical composition, which is given in Table I, corresponds to the commercial mid-alloy steel SAF 2205, which is to-day the most frequently produced duplex steel grade. The value of PREN factor was estimated within the range 35-38 on the base of the chemical composition, according to the formula;  $PREN = \%Cr + 3,3 (\%Mo) + k (\%N)$  [12, 13].

TABLE I  
The chemical composition of the examined duplex stainless steel (in weight %)

C	Cr	Ni	Mo	N	Mn	Si
0.02	22.28	6.05	2.95	0.19	1.72	0.51
Cu	Al	Nb	V	P	S	PREN
0.12	0.03	0.02	0.11	0.014	0.005	35

The material was received in the form of industrially hot-rolled sheets with the final thickness  $h_0 = 12.5$  mm. The preliminary thermo-mechanical treatment included additionally solution annealing conducted in laboratory conditions at the temperature 1150°C for 3 hours with subsequent water quenching.

The flat samples cut of the sheet were subjected to reversed rolling at room temperature on laboratory mill ( $\phi = 160$  mm) within the wide range of deformations, up to about 85% ( $\epsilon_t \approx 2$ ). Two cold-rolling variants were employed ( Fig.1 ) with rolling direction either perpendicular  $RD_C^1 \perp RD_H$  ( variant-1 ) or parallel  $RD_C^2 \parallel RD_H$  ( variant-2 ) to the direction of hot deformation. For both variants the same rolling schedule was adopted, which ensured the least strain gradient throughout the cross section in each roll-pass, i.e. with the ratio  $(L_c/h_m) > 1.0$ ; where  $L_c = \sqrt{R\Delta h}$  – the length of the arc of contact,  $R$  – radius of rolls,  $\Delta h$  – thickness reduction per pass and  $h_m$  – the mean thickness of the sheet. It is assumed that for such a rolling schedule the compressive strain penetrates throughout the whole thickness of the sheet in each roll-pass and a deformation rate of the centre layer, parallel to the rolling plane, is close to that of the subsurface layers [14].

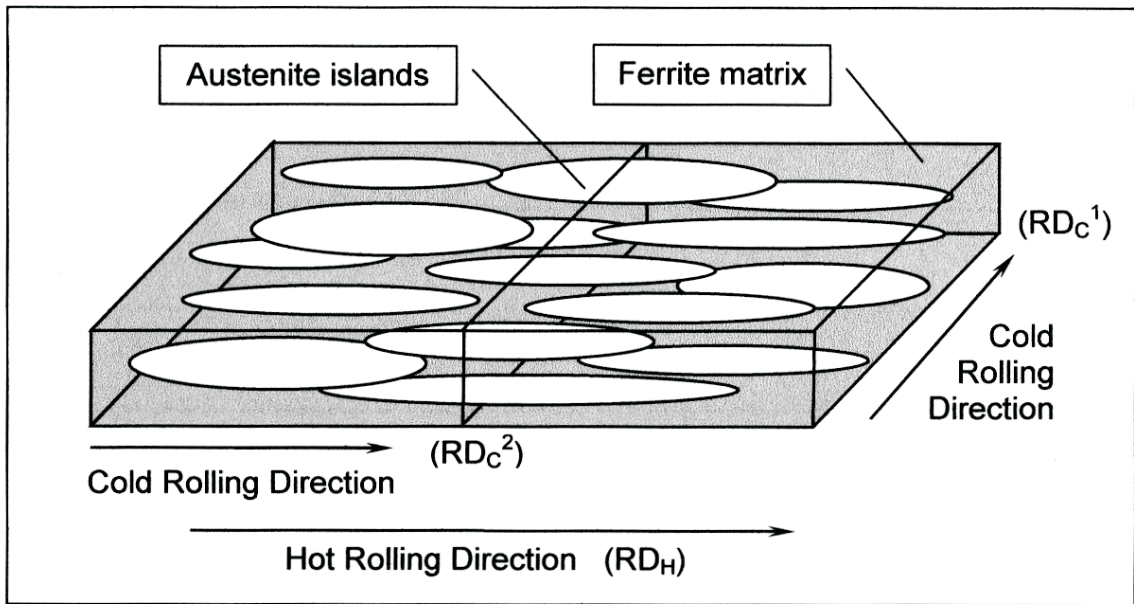


Fig. 1. Schematic illustration of the ferrite-austenite morphology after the thermo-mechanical pre-treatment and geometry of the applied cold-rolling variants;  $RD_C^1 \perp RD_H$  (variant-1) and  $RD_C^2 \parallel RD_H$  (variant-2)

Observations of the initial morphology of two-phase structure after hot-rolling and subsequent solution treatment as well as the changes of the ferrite-austenite band-like structure in the course of cold-rolling were conducted by means of optical microscopy (Neophot-2 and Axiovert-200 MAT microscopes). The phase composition of the steel and the ferrite-austenite morphology, were examined by means of the quantitative metallographic analysis employing program MET-ILO, version V.9.11 [15]. Details concerning the parameters adopted for microstructure characterisation are given by the present authors in earlier paper [12].

X-ray investigations were conducted by means of Bruker diffractometer D8 Advance, using Co  $K\alpha$  radiation ( $\lambda_{K\alpha}=0,179\text{nm}$ ). X-ray examination included the texture measurements and the phase analysis from the centre layers of the rolled sheets, for the initial state and within the wide range of rolling reductions. Texture analysis was based on the orientation distribution functions (ODFs) calculated from experimental (incomplete) pole figures recorded of three planes for each of the constituent phases, i.e. the  $\{110\}$ ,  $\{100\}$  and  $\{211\}$  planes for the bcc  $\alpha$ -phase and the  $\{111\}$ ,  $\{100\}$  and  $\{110\}$  planes for the fcc  $\gamma$ -phase. The values of the orientation distribution functions  $f(g)$  were examined along the typical orientation fibres;  $\alpha_1 = \langle 110 \rangle \parallel \text{RD}$ ,  $\gamma = \langle 111 \rangle \parallel \text{ND}$ ,  $\varepsilon = \langle 001 \rangle \parallel \text{ND}$  for ferrite and  $\alpha = \langle 110 \rangle \parallel \text{ND}$ ,  $\eta = \langle 001 \rangle \parallel \text{RD}$ ,  $\tau = \langle 110 \rangle \parallel \text{TD}$  for austenite.

Comparison of texture formation for both applied rolling variants was carried out after the selected rolling reductions on the basis of orientation distribution functions

(ODFs) as well as the  $\{111\}$  and  $\{110\}$  calculated pole figures, for austenite and ferrite respectively.

### 3. Results and discussion

#### 3.1. Initial morphology and starting textures

The morphology of two-phase structure in a ferritic-austenitic steel with a given chemical composition after preliminary thermo-mechanical treatment usually results from the applied type of hot-deformation process and the conditions of subsequent solution annealing, which determine the phase composition of a duplex type steel [3, 5, 12].

Schematic illustration of the ferrite-austenite morphology on the longitudinal and cross-sections of the sheet in duplex steel SAF 2205 after hot-rolling and after solution annealing at  $1150^\circ\text{C}$ , i.e. prior to cold-rolling in both variants, is shown in figures 2a÷c. Description of the ( $\alpha/\gamma$ ) two-phase microstructure after hot-rolling of the examined steel was given by the present authors elsewhere [12]. After solution annealing at the temperature  $1150^\circ\text{C} / 3$  hours certain noticeable changes in two-phase morphology were detected. The volume fractions of ferrite ( $V_V^F$ ) and austenite ( $V_V^A$ ) were estimated at about 60% and 40% respectively. Thus the ferritic  $\alpha$ -phase was more continuous and constituted the matrix with bands or elongated islands of the austenitic  $\gamma$ -phase. Pronounced directionality of the ferrite-austenite structure observed in hot-rolled sheet on the longitudinal ( $\text{ND}_H\text{-RD}_H$ ) section (Fig. 2a) remained essentially un-

changed after the solution treatment and the regions with considerable degree of banding still predominated (Figs. 2b,c). It should be noted however, that the areas of the  $\gamma$ -phase, which are arranged and elongated parallel to the hot-rolling direction  $RD_H$ , are less continuous after solution annealing. On the other hand the microstructure observed on the cross-sections ( $ND_H$ - $TD_H$ ) shows smaller structural anisotropy, i.e. significantly lower degree of banding and considerably smaller elongation parallel

the transverse direction  $TD_H$  (Figs. 2a÷c). In general the ( $\alpha/\gamma$ ) two-phase structure exhibits certain degree of heterogeneity, which concerns the distribution and arrangement as well as the size and shape of areas (grains) of both component phases. The exact description of the ferrite-austenite microstructure after solution treatment, employing quantitative image analysis, was given by the present authors in earlier paper [12].

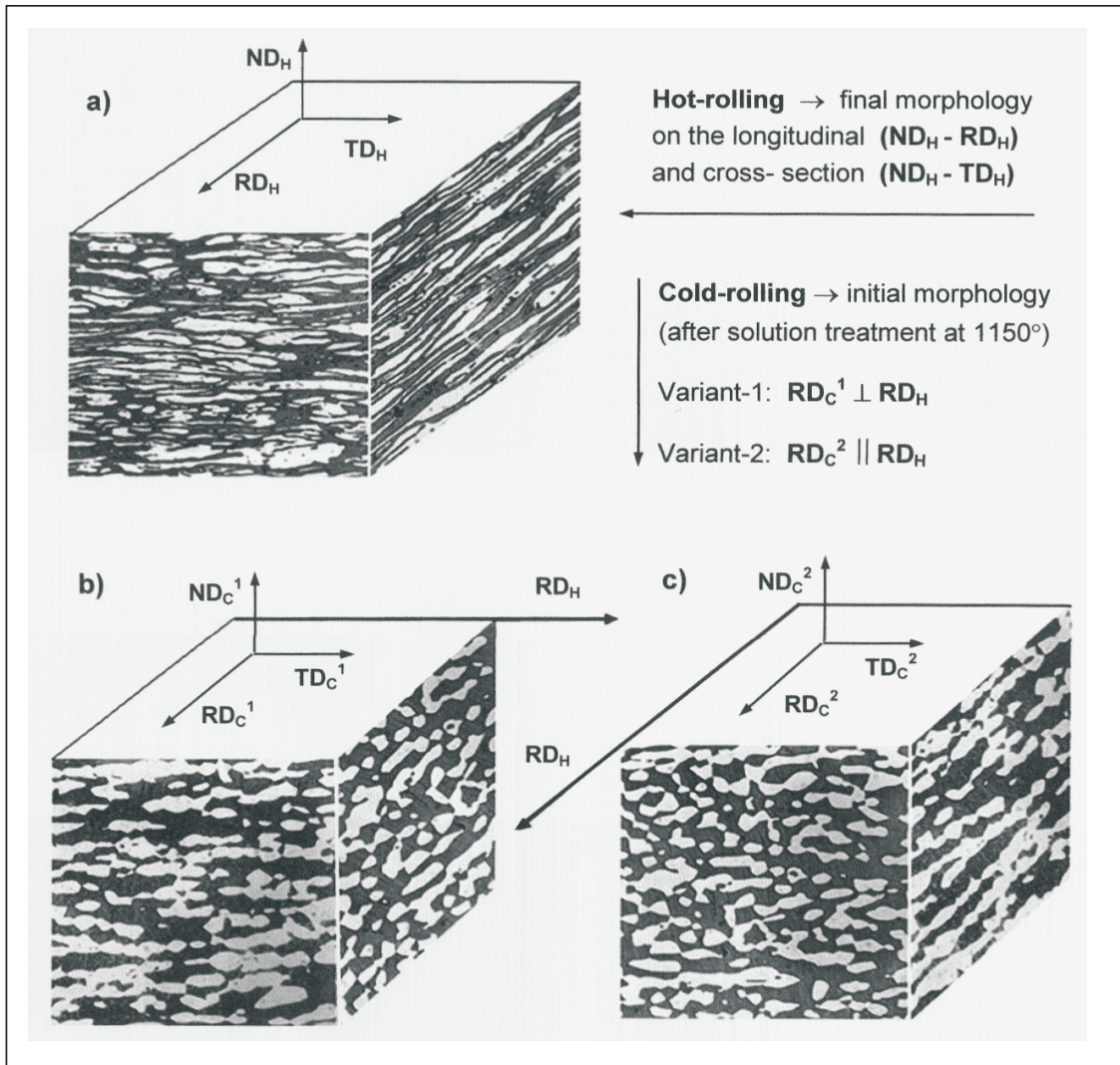


Fig. 2. Schematic illustration of the ferrite-austenite morphology after hot-rolling (a) and after solution annealing at 1150°C, prior to cold-rolling in variant-1 (b) and variant-2 (c) on the longitudinal and cross-sections of the sheet

Texture measurements conducted after hot-rolling revealed relatively weak textures in both constituent phases (Fig. 3a). The texture of ferrite showed partially fibrous character with orientations  $\{001\}\langle 100 \div 110 \rangle$  and the maximum intensity  $f(g)=3.2$  corresponding to

the component close to the  $\{001\}\langle 320 \rangle$  orientation, whereas the major component of the austenite texture was the  $\{001\}\langle 100 \rangle$  cubic orientation with the intensity  $f(g)=2.3$ .

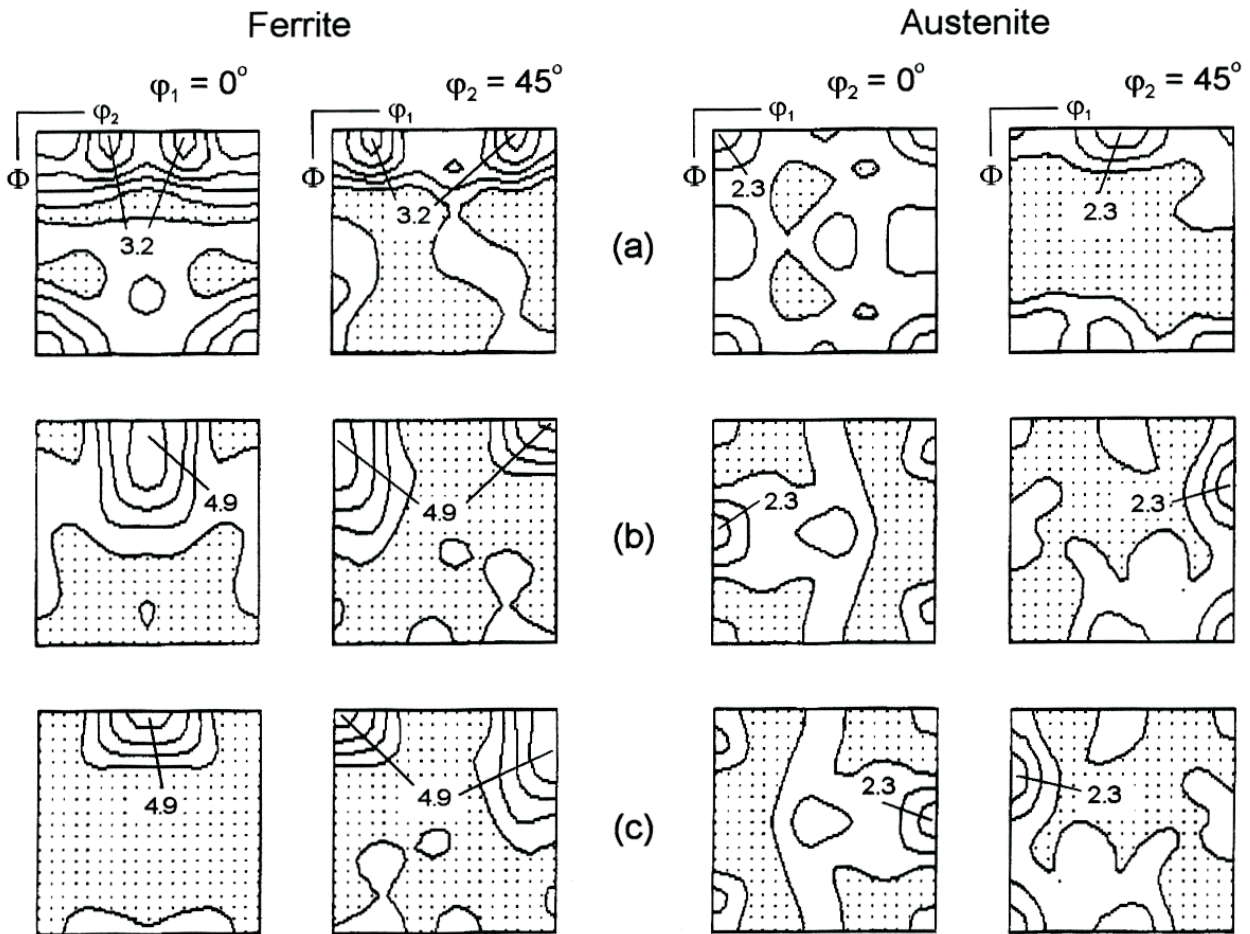


Fig. 3. Orientation distribution functions (ODFs) in sections  $\varphi_1 = 0^\circ$ ,  $\varphi_2 = 45^\circ$  for ferrite and  $\varphi_2 = 0^\circ$ ,  $\varphi_2 = 45^\circ$  for austenite, from the centre layer of the sheet; (a) – after hot-rolling, (b) – after solution annealing (starting texture for variant-2), and (c) – after 90°/ND rotation (starting texture for variant-1)

After solution treatment at 1150°C / 3h the texture of austenite remained very weak (Fig. 3b). The major texture component with the intensity  $f(g)=2.3$ , which is the Goss orientation  $\{110\}\langle 001\rangle$ , was observed against the background of nearly random texture. The texture of ferrite after solution annealing was stronger with the maximum intensity  $f(g)=4.9$  corresponding to the  $\sim\{114\}\langle 110\rangle$  orientation, which is deviated about 20° from the rotated cubic  $\{001\}\langle 110\rangle$  component having approximate intensity. The ferrite texture may be essentially described by the limited fibres;  $\alpha_1 = \langle 110\rangle \parallel \text{RD}$  and  $\varepsilon = \langle 001\rangle \parallel \text{ND}$ . These are the starting orientation distributions for the rolling variant-2 (Fig. 1), i.e. for cold-rolling parallel to the direction of hot-deformation,  $\text{RD}_C^2 \parallel \text{RD}_H$ .

In the case of the rolling variant-1 the samples cut of the hot-rolled sheet were subjected to cold-rolling perpendicularly to the direction of hot-deformation,  $\text{RD}_C^1 \perp \text{RD}_H$  (Fig. 1). That is why the starting orientation distributions of both constituent phases were changed with

respect to the external co-ordinate system due to the rotation of the samples 90° around the ND direction, normal to the sheet. After 90° / ND rotation, the strongest component of the initial texture of ferrite was the rotated cubic orientation  $\{001\}\langle 1\bar{1}0\rangle$  and the maximum intensity of the austenite starting texture corresponded to the  $\{110\}\langle 1\bar{1}0\rangle$  orientation (Fig. 3c).

Schematic illustrations of the strongest components of the austenite and ferrite starting textures together with the stereographic projections of the potential slip systems in both component phases are shown in figures 4 and 5 respectively, for both variants of cold-rolling. Estimation of the most stressed slip systems within the textured ferrite-austenite banded structure was carried out based on the calculation of the relative shear stresses, i.e. the ratios  $m = (\tau/\sigma)$ , for the strongest components in the starting textures of both phases.

When comparing the initial orientation distributions for both rolling variants it should be noted that ferrite exhibits a very specific texture after pre-treatment. The ma-

major components of the ferrite starting textures are of the same type, i.e. the  $\{001\}\langle 110\rangle$  and  $\{001\}\langle 1\bar{1}0\rangle$  rotated cubic orientations. Additionally very similar is the texture spread along the  $\varepsilon = \langle 001\rangle \parallel \text{ND}$  fibre and the only essential difference is the character of the  $\alpha_1 = \langle 110\rangle \parallel \text{RD}$  fibre (Fig. 3b,c). For major orientation components

of the initial texture the highest values of the relative shear stresses are in two  $\{112\}\langle 111\rangle$  slip systems ( $m = 0,942$ ) and four  $\{110\}\langle 111\rangle$  slip systems ( $m = 0,816$ ) and these potential slip systems are symmetrical with respect to the cold-rolling directions  $\text{RD}_C^2 \parallel \langle 110\rangle$  and  $\text{RD}_C^1 \parallel \langle 1\bar{1}0\rangle$  (Fig. 4).

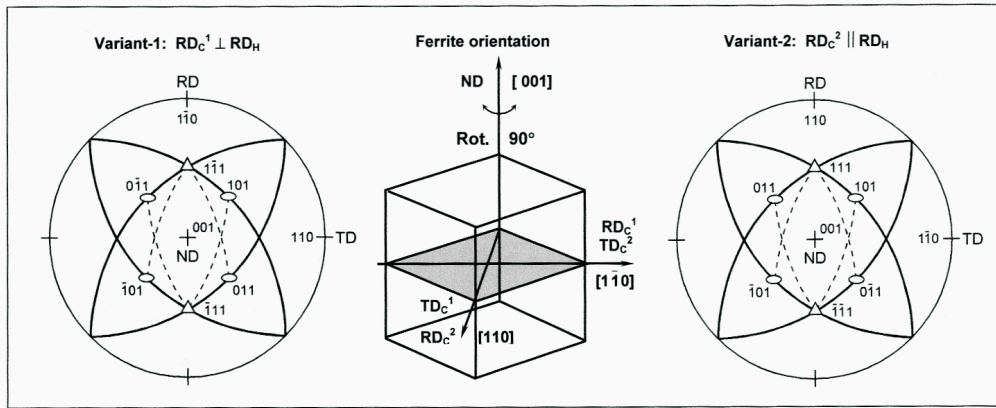


Fig. 4. Schematic illustration of the strongest component of the ferrite starting texture and the stereographic projections of the potential slip systems for both variants of cold-rolling

In austenite the initial orientation distributions for both rolling variants are quite different. For the  $\{110\}\langle 001\rangle$  Goss orientation, as the strongest component in variant-2 ( $\text{RD}_C^2 \parallel \text{RD}_H$ ), the highest values of the relative shear stresses are in two  $\{111\}\langle 112\rangle$  twin systems ( $m = 0,942$ ) and four  $\{111\}\langle 110\rangle$  slip systems ( $m = 0,816$ ). On the other hand for the major texture component  $\{110\}\langle 1\bar{1}0\rangle$  in variant-1 ( $\text{RD}_C^1 \perp \text{RD}_H$ ) there are four  $\{111\}\langle 112\rangle$

equally stressed twin systems ( $m = 0,471$ ) and eight  $\{111\}\langle 110\rangle$  slip systems ( $m = 0,408$ ). Obviously not all of these systems are active simultaneously (Fig. 5). It is assumed that the specific morphology of two-phase structure forces the operation of the selected slip systems, symmetrical with respect to  $\text{RD}_C$ , which ensure compatible deformation of the ferrite and austenite bands (layers) [4, 5].

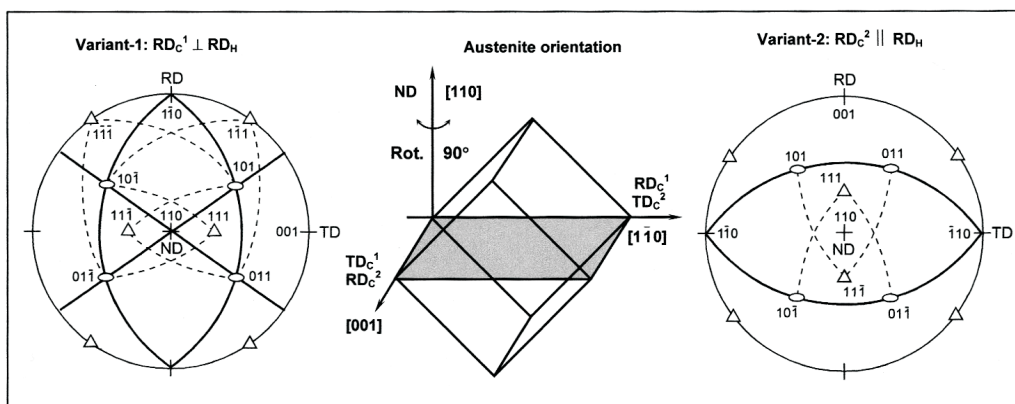


Fig. 5. Schematic illustration of the strongest component of the austenite starting texture and the stereographic projections of the potential slip systems for both variants of cold-rolling

### 3.2. Texture and microstructure after cold-rolling

Changes in the morphology of the ferrite-austenite microstructure for both rolling variants, as observed

on the longitudinal ( $\text{ND}_C\text{-RD}_C$ ) and cross-sections ( $\text{ND}_C\text{-TD}_C$ ) of the cold-rolled samples, are shown after 30% and 70% of reduction in figures 6a,b and 7a,b respectively. It should be noted, that in the

case of the rolling variant-1 ( $RD_C^1 \perp RD_H$ ) the initial two-phase morphology observed on the longitudinal section ( $ND_C-RD_C$ ) corresponded to that on the cross-section ( $ND_H-TD_H$ ) of the hot-rolled sheet, i.e. before  $90^\circ$  /ND rotation. This is clearly visible when comparing ferrite-austenite morphology after 30% of reduction for both rolling variants (Fig. 6a,b). For the rolling variant-1 the elongation of the austenite areas on the longitudinal section ( $ND_C-RD_C$ ) is still smaller in comparison to that observed on the cross-section ( $ND_C-TD_C$ ). On the contrary, for the rolling variant-2 there is a continuation in elongation of the ferrite and austenite bands parallel to both rolling directions ( $RD_C^2 \parallel RD_H$ ). In the course of cold-rolling the component phases were plastically deformed and formed characteristic band-like structure (so-called pancake structure) consisting of alternate bands (flat shapes) of ferrite and austenite arranged and elongated parallel to the rolling plane. With the increas-

ing rolling reduction a significant refinement of the microstructure was observed, with the thickness reduction of the austenite bands to about few micrometers [1÷6]. The layers of ferrite were thicker and exhibited more continuous character due to the phase composition of the steel (Figs. 6a,b and 7a,b). When comparing changes in morphology of two-phase structure for both rolling variants it should be noted that within the range of medium strains, i.e. 50%-60% of reduction, the microstructure of the examined steel SAF 2205 exhibits considerably smaller structural anisotropy for the case of cold-rolling variant-1 ( $RD_C^1 \perp RD_H$ ), that is to say smaller differences in elongation of the second phase (austenite) as observed on both sections of the cold-rolled sheet. A comparable morphology of the ferrite-austenite microstructure for both cold-rolling variants on the longitudinal and cross-sections of the sheets is starting to be observed from about 70% of reduction (Fig. 7a,b).

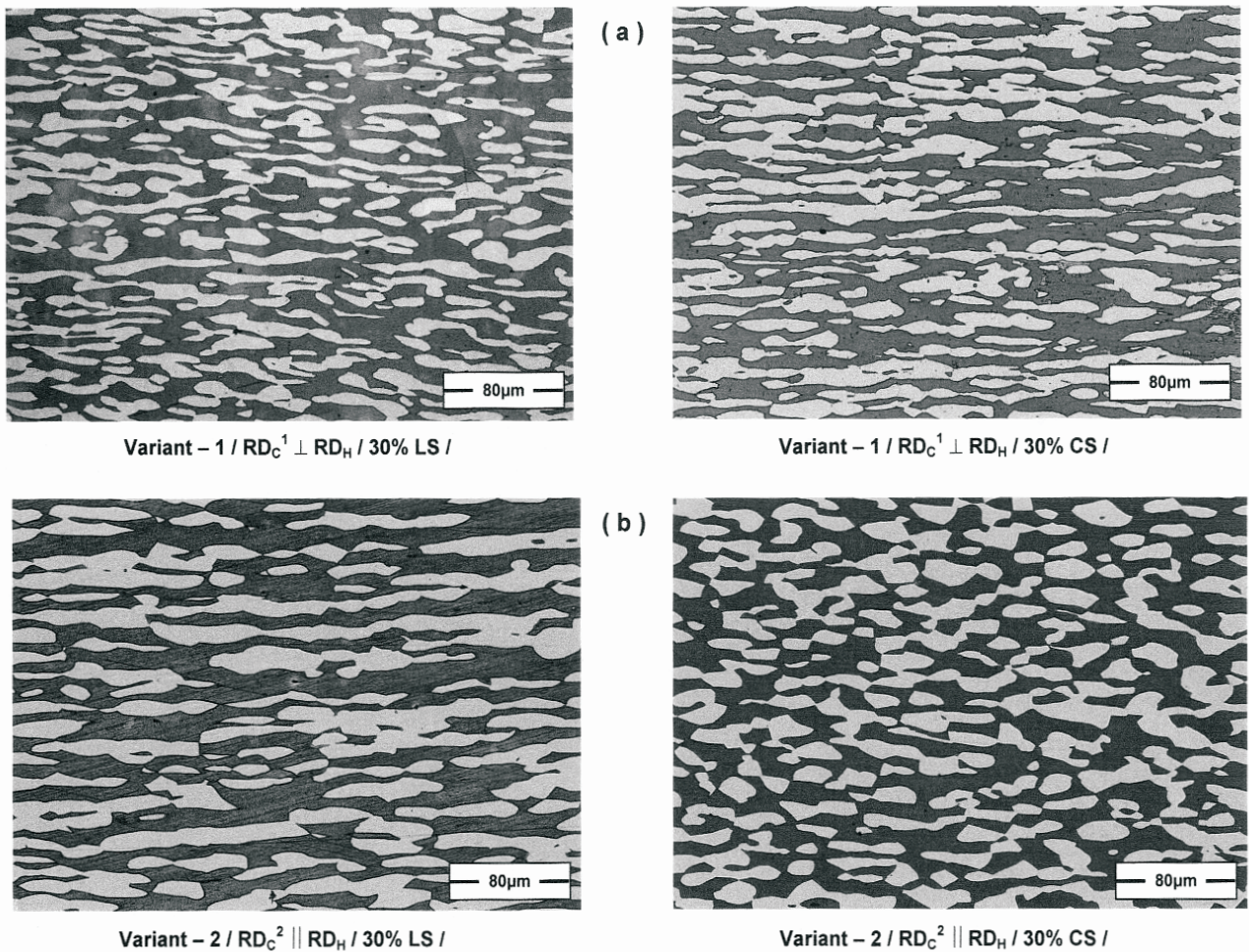


Fig. 6. The morphology of the ferrite-austenite microstructure after 30% of deformation on the longitudinal and cross sections of the rolled sheet; (a) – rolling variant-1 ( $RD_C^1 \perp RD_H$ ) and (b) – rolling variant-2 ( $RD_C^2 \parallel RD_H$ )

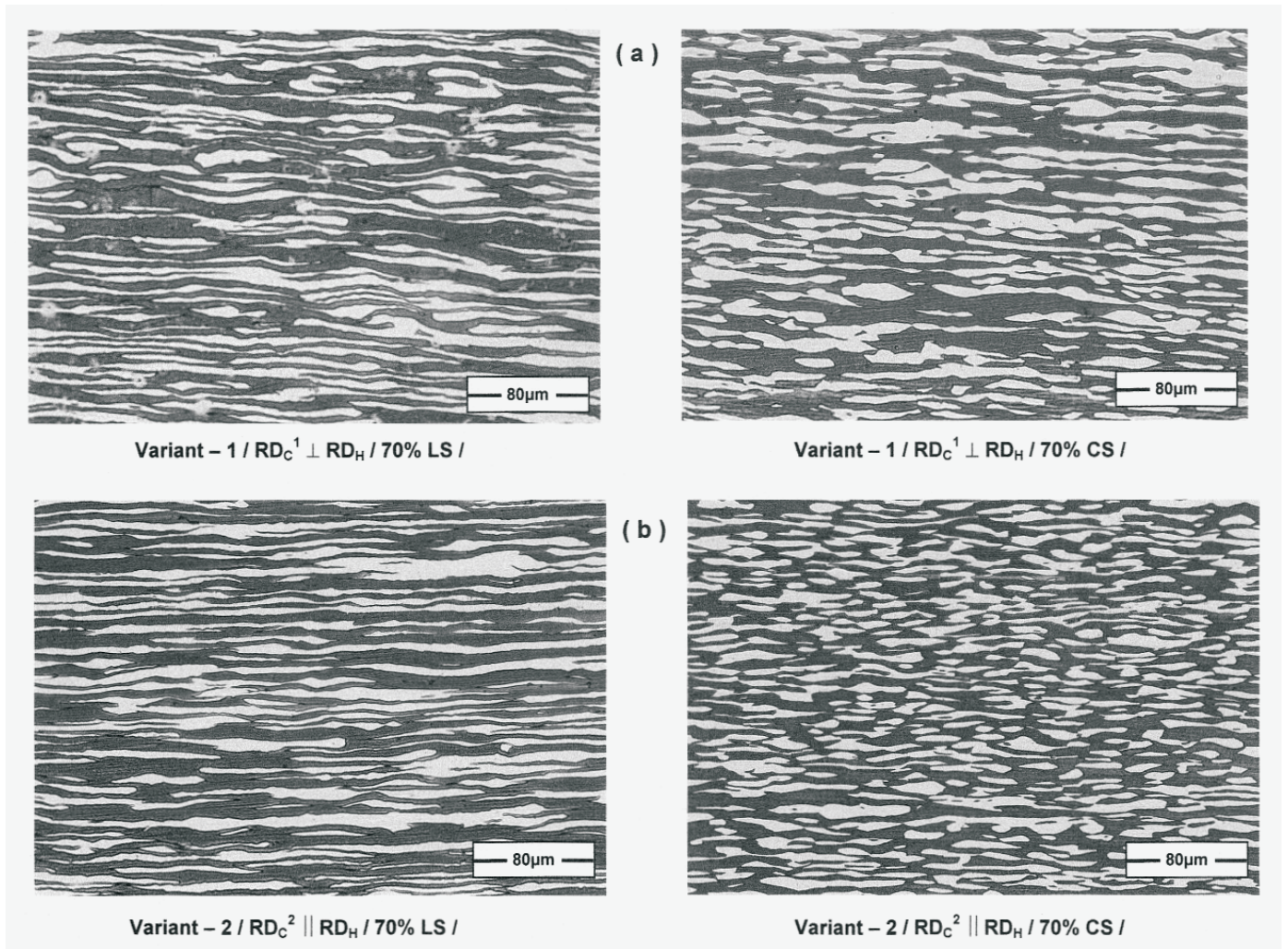


Fig. 7. The morphology of the ferrite-austenite microstructure after 70% of deformation on the longitudinal and cross sections of the rolled sheet; (a) – rolling variant-1 ( $RD_C^1 \perp RD_H$ ) and (b) – rolling variant-2 ( $RD_C^2 \parallel RD_H$ )

The measurements of the ferrite and austenite deformation textures carried out in the course of cold-rolling revealed quite different behaviour of both constituent phases, which is especially pronounced in the case of the rolling variant-1 ( $RD_C^1 \perp RD_H$ ). Texture changes after the successive rolling reductions were analysed in the selected one-dimensional sections through the ODFs (Figs. 8 and 10) along the orientations fibers characteristic for both, fcc and bcc phases [1÷3]. Additional examination concerned the calculated pole figures,  $\{110\}$  for ferrite and  $\{111\}$  for austenite, after the selected rolling reductions (Figs. 9 and 11).

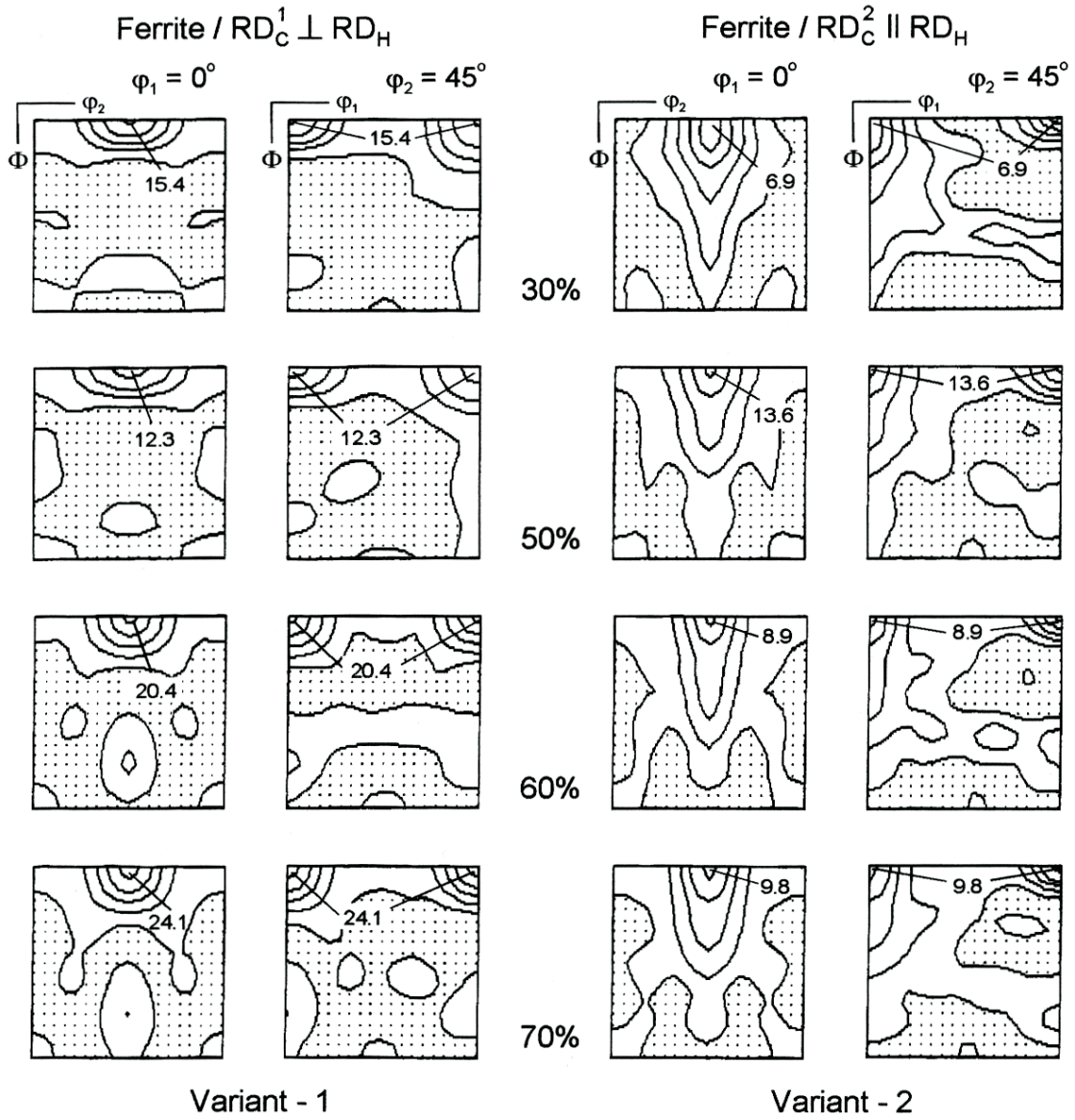


Fig. 8. Orientation distribution functions (ODFs) for ferrite in sections  $\varphi_1 = 0^\circ$  and  $\varphi_2 = 45^\circ$  after the selected thickness reductions for both rolling variants (centre layers of the sheet)

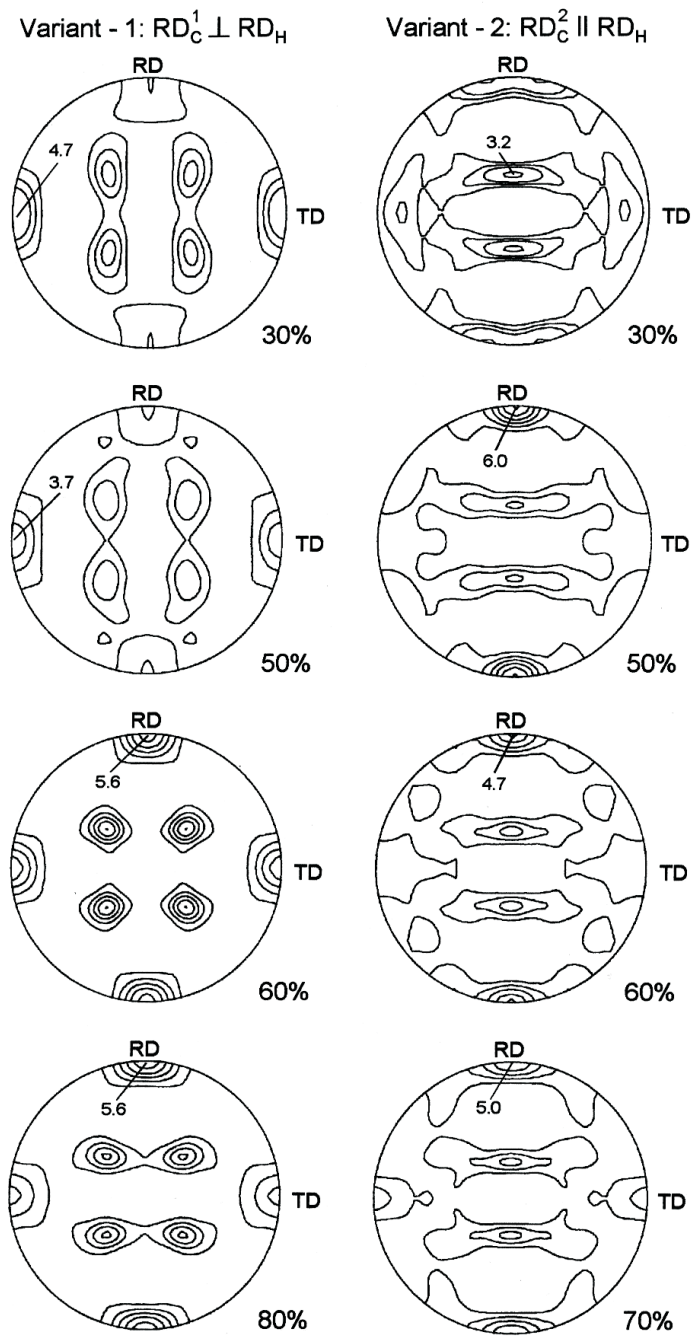


Fig. 9. Comparison of the calculated  $\{110\}$  pole figures of ferrite after the selected rolling reductions for both rolling variants

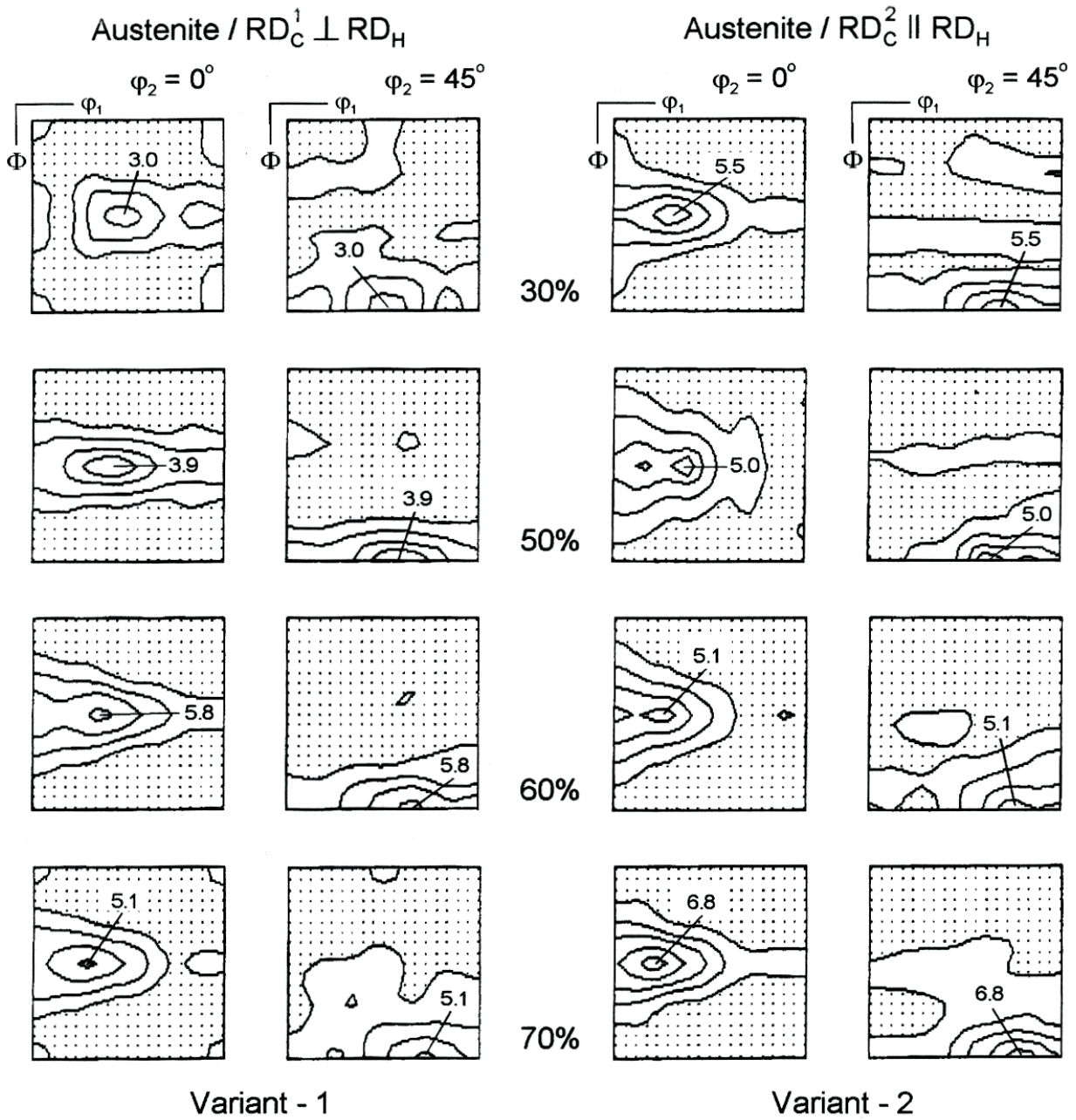


Fig. 10. Orientation distribution functions (ODFs) for austenite in sections  $\varphi_2 = 0^\circ$  and  $\varphi_2 = 45^\circ$  after the selected thickness reductions for both rolling variants (centre layers of the sheet)

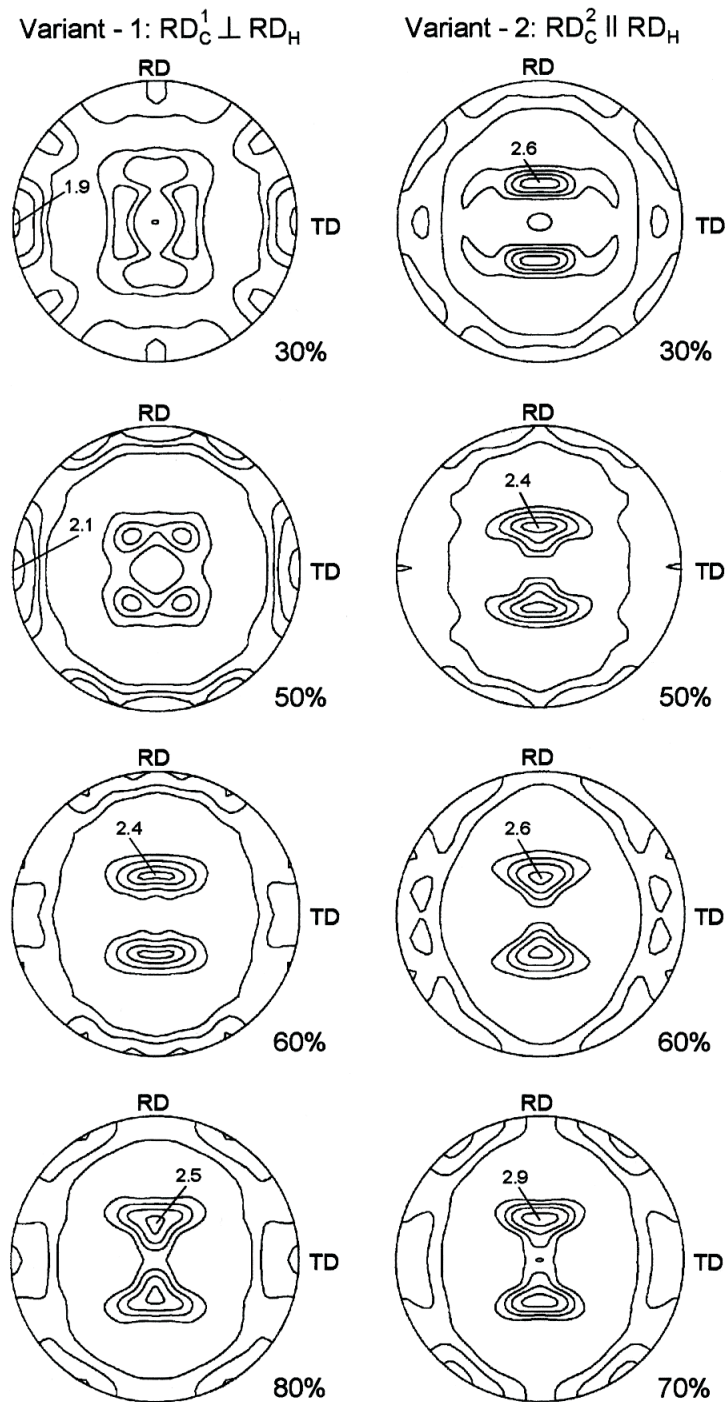


Fig. 11. Comparison of the calculated  $\{111\}$  pole figures of austenite after the selected rolling reductions for both rolling variants

In the case of ferrite there are certain differences in the character of textures between both rolling variants. However these differences do not concern the major texture components, which are of the same type, but the extension of texture spread along the  $\alpha_1$ -fibre and the intensities of orientations located within the spread of major components (Fig. 8).

For the rolling variant-1 the ferrite rolling texture exhibits relatively high stability. The major component of the initial texture, i.e. the  $\{001\}\langle 110 \rangle$  orientation, occurred the dominant orientation within the whole range of deformations. The rotated cubic orientation  $\{001\}\langle 110 \rangle$  from the  $\varepsilon = \langle 001 \rangle \parallel \text{ND}$  and  $\alpha_1 = \langle 110 \rangle \parallel \text{RD}$  fibers is one of the typical components of ferrite

rolling textures. Basically the only changes in the ferrite rolling texture, as observed in ODF sections  $\varphi_1 = 0^\circ$  and  $\varphi_2 = 45^\circ$  (Fig. 8), concerned the orientation components of weaker intensities from the  $\alpha_1$ - and  $\varepsilon$ -fibers. In general the inhomogeneous and limited  $\varepsilon$ -fiber was observed within the whole range of deformations. On the other hand the texture spread along the  $\Phi$  direction showed relatively small extension and the limited and very inhomogeneous  $\alpha_1$ -fiber appeared only at higher deformations, starting from about 60% of reduction. The maximum texture intensity was relatively high, reaching the value  $f(g)=24$  after 70% of deformation.

Also in the case of the rolling variant-2 the ferrite texture remained essentially unchanged over the wide range of deformations. The dominant texture component occurred once again the  $\{001\}\langle 1\bar{1}0 \rangle$  rotated cubic orientation (Fig. 8). The major difference in comparison to the rolling variant-1 was the character of the  $\alpha_1$ -fiber, which is clearly more extended along the  $\Phi$  direction, however very inhomogeneous with the maximum intensity corresponding to the major component  $\{001\}\langle 1\bar{1}0 \rangle$ . Similarly to the rolling variant-1 only slight fluctuations in the extension of the limited and inhomogeneous  $\varepsilon$ -fiber were observed with increasing deformation degree. In general the intensity of ferrite texture for the rolling variant-2 was significantly smaller (Fig. 8).

A striking difference between the ferrite rolling textures of the examined duplex steel (Fig. 8) in comparison to one-phase ferritic steels is the absence of the  $\gamma = \langle 111 \rangle \parallel$  ND fiber in the case of rolling variant-1 and its very weak representation in the course of deformation for the rolling variant-2 [3,10]. It results apparently from the stability of the dominant  $\{001\}\langle 110 \rangle$  components and very small or relatively low texture spread for both rolling variants upon deformation.

Stability of the dominant components of the ferrite texture after the selected rolling reductions is very well visible on the calculated  $\{110\}$  pole figures for both variants of cold-rolling (Fig. 9). However, comparison of the texture formation for both variants indicates at a different character of the pole figures concerning the orientation distribution for minor texture components. The characteristic rearrangement of texture spread in the case of rolling variant-1, which initially was parallel and finally perpendicular to the rolling direction  $RD_C$ , is the effect of orientation changes resulting from the  $90^\circ$  rotation of the samples around the ND, i.e. the change of the rolling direction,  $RD_C^1 \perp RD_H$  (Fig. 1).

In contrast to ferrite, a gradual development of the final austenite rolling texture was observed in the case of the rolling variant-1 within the relatively wide range of deformations (Fig. 10). Due to  $90^\circ/ND$  rotation of the sheet the major component of austenite starting texture

was the  $\{110\}\langle 1\bar{1}0 \rangle$  orientation (Fig. 3c). After 30% of reduction the limited  $\{110\}\langle uvw \rangle$  fibre was formed, with the maximum intensity  $f(g)=3.0$  corresponding to the  $\sim\{110\}\langle 223 \rangle$  and  $\sim\{110\}\langle 441 \rangle$  orientations. At medium deformations, i.e. about 50% of rolling reduction, the inhomogeneous and extended  $\alpha = \langle 110 \rangle \parallel$  ND fibre was formed with maximum intensities shifting from the  $\{110\}\langle 112 \rangle$  to the  $\{110\}\langle 111 \rangle$  orientations. Starting from about 60% of reduction the austenite rolling texture is relatively stable and may be described by the limited  $\alpha$ -fibre with the maximum shifting within the range  $\{110\}\langle 113 \div 112 \rangle$ . Additionally a certain contribution of the components from the limited and inhomogeneous  $\eta = \langle 001 \rangle \parallel$  RD fibre is observed at higher strains. It appears however that the intensity for the  $\{110\}\langle 001 \rangle$  Goss orientation is considerably smaller in comparison to a number of cold-rolled one-phase austenitic steels [2,11]. Within the whole range of deformations the orientation densities for the austenite texture were rather low, i.e.  $f(g)=3.0 \div 5.8$ . At about 70% of deformation the rolling texture of austenite is close to the alloy-type texture, which is typical for low SFE materials including one-phase austenitic steels [11].

On the other hand for the rolling variant-2 the strongest component of the austenite starting texture was the  $\{110\}\langle 001 \rangle$  Goss orientation (Fig. 3b). The limited  $\alpha = \langle 110 \rangle \parallel$  ND fibre with the maximum intensity  $f(g)=5.5$  corresponding to the  $\sim\{110\}\langle 112 \rangle$  alloy type orientation was formed already after about 30% of reduction. Afterwards the texture was relatively stable and may be additionally described by the limited and inhomogeneous  $\eta = \langle 001 \rangle \parallel$  RD fibre (Fig. 10).

Examination of the texture development in austenite, based on the calculated  $\{111\}$  pole figures, indicates at the formation of an alloy type texture for both rolling variants (Fig. 11). In the case of cold-rolling conducted parallel to direction of hot deformation (variant-2) the texture close to the  $\{110\}\langle 112 \rangle$  alloy type texture started to develop already at about 30% of deformation. On the other hand after  $90^\circ/ND$  rotation, i.e. for cold-rolling variant-1 conducted perpendicularly to the austenite bands elongated parallel to the hot-rolling direction ( $RD_H$ ), the initial texture of austenite was gradually changing within the wide range of deformations and reached the form of an alloy type texture not before the final deformation stages, i.e. at about 80% of reduction. It should be noted that due to the elemental partitioning during the high temperature annealing the concentration of nitrogen in austenite is frequently estimated at about 90% [13]. Taking into account the 0.19% addition of nitrogen, annealing at  $1150^\circ\text{C}$  for 3 hours and austenite volume fraction  $V_V^A = 40\%$ , the nitrogen contents within the  $\gamma$ -phase may even exceed 0.4% in the examined

steel [12]. The fact that higher concentrations of nitrogen (above ~0.4% N) strongly decrease the SFE value of austenite seems to account for the formation of an alloy type textures even in thin austenite bands within the ferrite matrix [1, 3, 6].

#### 4. Concluding remarks

The present research concerns the texture formation in the ferritic-austenitic steel SAF 2205 of duplex type, which was cold-rolled after the preliminary thermo-mechanical treatment perpendicularly ( $RD_C^1 \perp RD_H$ ) and parallel ( $RD_C^2 \parallel RD_H$ ) to the direction of hot-rolling. Texture analysis indicates that regardless of the applied cold-rolling variant austenite shows tendency to develop the textures close to those in one-phase austenitic steels and the final rolling textures of ferrite significantly differ from those in single phase ferritic steels.

The rotation of the sheet  $90^\circ$  around the normal direction ND, did not essentially change the type of the major component in the ferrite starting texture, which in both cases was of the  $\{001\}\langle 110 \rangle$  type, i.e. rotated cubic orientation. Thus ferrite showed a very specific initial orientation distribution after preliminary treatment. On the contrary, in austenite there was considerable orientation change with respect to the new co-ordinate system and the strongest components of the starting textures were as follows; the  $\{110\}\langle 1\bar{1}0 \rangle$  orientation for variant-1 ( $RD_C^1 \perp RD_H$ ) and the  $\{110\}\langle 001 \rangle$  Goss orientation in the case of variant-2 ( $RD_C^2 \parallel RD_H$ ).

The major component of the ferrite starting texture, i.e. the  $\{001\}\langle 110 \rangle$  rotated cubic orientation, was stable up to high deformations for both cold-rolling variants. Similarly the character of texture spread, which was different for both variants, remained essentially unchanged over the whole deformation range. Only slight changes of the limited  $\alpha_1$ - and  $\epsilon$ -fibers with strong  $\{001\}\langle 110 \rangle$  component were detected, especially in the case of the rolling variant-2 ( $RD_C^2 \parallel RD_H$ ). In general the only changes within the ferrite rolling textures in the course of cold-rolling concerned the minor orientations from the texture spread, that is components of weaker intensities. Very characteristic feature of the texture formation in ferrite was the absence of the  $\gamma$ -fiber for the case of the rolling variant-1 and its very weak representation upon rolling in variant-2.

In the austenitic phase a gradual formation of the final textures was observed, for both employed rolling variants. For the case of rolling variant-2 ( $RD_C^2 \parallel RD_H$ ) the texture close to the  $\{110\}\langle 112 \rangle$  alloy-type texture started to form already after about 30% of deformation. On the contrary in variant-1 ( $RD_C^1 \perp RD_H$ ) the orien-

tation changes proceeded over the wide range of rolling reductions. The fact that austenite is the second phase ( $V_V^A = 40\%$ ) in the form of thin bands within the ferrite matrix significantly restrains lattice rotations. That is why the resulting orientation changes were extended over a wide deformation range and the intensity of the final rolling texture occurred relatively low. However, the addition of nitrogen and its concentration mainly within the  $\gamma$ -phase considerably decreased stacking fault energy and as the result austenite finally reached the rolling texture close to that in low SFE alloys.

Another noticeable difference between the rolling textures of the constituent phases is the texture intensity, i.e. the orientation density  $f(g)$  for the main texture components. However the texture intensity of austenite increased somewhat at higher deformations, nevertheless remained relatively low. Over the whole deformation range the intensities of the ferrite rolling textures were found to be considerably higher in comparison to the orientation density in austenite. This difference results not only from the phase composition of the steel after the preliminary treatment ( $V_V^F = 60\%$  and  $V_V^A = 40\%$ ) but from the initial morphology of two-phase structure as well.

Very important conclusion results from the juxtaposition of the ferrite textures and the austenite textures for both rolling variants with microstructure observations concerning the morphology of two-phase structure observed on both sections of the rolled sheets. Within the range of medium strains, i.e. 50%-60% of reduction, the microstructure of the examined steel exhibits considerably smaller structural anisotropy for the case of cold-rolling variant-1 ( $RD_C^1 \perp RD_H$ ), that is to say smaller differences in elongation of the second phase (austenite) as observed on both sections of the cold-rolled sheet. On the other hand the textures of austenite as well as ferrite exhibit very similar character for both rolling variants within the same deformation range. These are the textures of the same or very close major components, which essentially differ only in the texture spread, i.e. the occurrence and the intensity of minor orientations. This result seems to indicate, that anisotropy of a number of mechanical properties usually observed in duplex steels sheets arises not only from the specific band-like morphology of two-phase structure but essentially is the consequence of the rolling textures which developed within both component phases.

In general it is concluded that the initial band-like morphology of the ferrite-austenite microstructure and the starting textures of both component phases after the preliminary treatment exert significant influence on the formation of the final textures upon subsequent cold-rolling of the examined duplex steel. This re-

sult indicates at the importance of the conditions for thermo-mechanical processes, which produce specific morphology and preferential orientation distributions prior to cold-rolling of ferritic-austenitic steels.

#### Acknowledgements

The authors wish to thank Prof. W. Ratuszek for invaluable help and stimulating discussions. The work was financially supported by the Polish Committee for Scientific Research (KBN) under the contract No. 10.10.110.720.

#### REFERENCES

- [1] N. Akdut, J. Foct, Phase Boundaries and Deformation in High Nitrogen Duplex Stainless Steels, I – Rolling Texture Development & II – Analysis of Deformation Mechanisms by Texture Measurements, *Scripta Metall. et Mater.* **32**, 103-108, 109-114 (1995).
- [2] N. Akdut, J. Foct, G. Gottstein, Cold Rolling Texture Development of ( $\alpha/\gamma$ ) Duplex Stainless Steel, *Steel Research* **67**, 450-455 (1996).
- [3] J. Keichel, J. Foct, G. Gottstein, Deformation and Annealing Behaviour of Nitrogen Alloyed Duplex Stainless Steels. Part I: Rolling, *ISIJ International*. **43**, 1781-1787 (2003).
- [4] J. Ryś, W. Ratuszek, M. Witkowska, The Effect of Initial Orientation and Rolling Schedule on Texture Development in Duplex Steel, *Materials Science Forum* **495-497**, 375-380 (2005).
- [5] J. Ryś, W. Ratuszek, M. Witkowska, Rolling Texture Differences in Duplex Steels with Strong and Random Initial Textures, *Solid State Phenomena* **130**, 57-62 (2007).
- [6] J. Ryś, M. Witkowska, Rolling Texture Development in Nitrogen Alloyed Ferritic-Austenitic Steel of Duplex Type, *Archives of Metallurgy and Materials* **53**, 221-228 (2008).
- [7] J. J. Moverare, M. Oden, Influence of Elastic and Plastic Anisotropy on the Flow Behaviour in a Duplex Stainless Steel, *Metall. and Mater. Trans. A*, **33 A**, 57-71 (2002).
- [8] J. L. Song, P. S. Bate, Plastic Anisotropy in a Superplastic Duplex Stainless Steel, *Acta Materialia* **45**, 2747-2757, (1997).
- [9] W. B. Hutchinson, K. Ushioda, G. Runnsjö, Anisotropy of Tensile Behaviour in a Duplex Stainless Steel Sheet, *Mater. Science and Techn.* **1**, 728-731 (1985).
- [10] D. Raabe, K. Lücke, Textures of Ferritic Stainless Steels, *Mater. Science and Techn.* **9**, 302-312 (1993).
- [11] D. Raabe, Texture and Microstructure Evolution during Cold Rolling of a Strip Cast and of a Hot Rolled Austenitic Stainless Steel, *Acta Materialia* **45**, 1137-1151 (1997).
- [12] J. Ryś, M. Witkowska, P. Matusiewicz, The Effect of Solution Treatment and Nitrogen Addition on Phase Composition of Duplex Steels, *Archives of Metallurgy and Materials* **53**, 229-236 (2008).
- [13] Weber, P. J. Uggowitzer, Partitioning of Chromium and Molybdenum in Super Duplex Stainless Steels with Respect to Nitrogen and Nickel Content, *Mater. Sci. & Eng.* **A242**, 222-229 (1998).
- [14] Tselikov, *Stress and Strain in Metal Rolling*, Mir Publishers, Moscow (1967).
- [15] J. Szala, Zastosowanie metod komputerowej analizy obrazu do ilościowej oceny struktury materiałów, *Zeszyty Naukowe Politechniki Śląskiej*, 61 (2001).